Title

INFLUENCE OF MICRO STRUCTURAL FEATURES ON FRACTURE TOUGHNESS OF AN ULTRA-HIGH STRENGTH STEEL

Authors

Lai, G.Y.
Wood, W.E.
Parker, E.R.
et al.

Publication Date

1975-04-01

LBL-2236
Preprint

INFLUENCE OF MICROSTRUCTURAL FEATURES ON FRACTURE TOUGHNESS OF AN ULTRA-HIGH STRENGTH STEEL

G. Y. Lai, W. E. Wood, E. R. Parker, and V. F. Zackay

April 1975

Prepared for the U. S. Energy Research and Development Administration under Contract W-7405-ENG-48

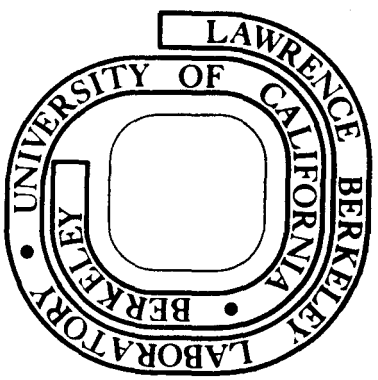

DISCLAIMER

INFLUENCE OF MICROSTRUCTURAL FEATURES ON FRACTURE TOUGHNESS OF AN ULTRA-HIGH STRENGTH STEEL

G. Y. Lai, W. E. Wood, E. R. Parker and V. F. Zackay

Inorganic Materials Research Division, Lawrence Berkeley Laboratory and Department of Materials Science and Engineering, College of Engineering' University of California, Berkeley, California 94720

ABSTRACT

Superior toughness at a high strength level was obtained for AISI 4340 steel by a new heat treatment (austenitizing at 1200°C followed by cooling to 870°C before quenching) which is different from the conventional heat treatment (austenitizing at 870°C). The steel with two different heat treatments was studied in terms of plane strain fracture toughness, fracture mode and microstructure. Characterization of microstructure was carried out by both optical microscopy and thin foil transmission electron microscopy. Results show that a significant improvement in fracture toughness at a similar high level of yield strength can be obtained in both the as-quenched and low-temperature tempered conditions when the austenitizing temperature is raised from 870°C to 1200°C. This improvement in fracture toughness using the 1200°C austenitizing temperature was attributed to (a) the elimination or at least minimization of twinned martensite plates, and (b) the large increase in the amount of retained austenite films which surround martensite laths.

When the specimens, following austenitizing at 870°C (resulting in the austenite grain size ASTM 7-8) were tempered, there was no evidence of tempered martensite embrittlement in the room temperature plane strain fracture toughness measurements. However, the embrittlement

was observed after tempering at 280°C and 350°C in specimens that were austenitized at 1200°C (resulting in the austenite grain size ASTM 0-1). The distribution and morphology of cementite platelets both at lath boundaries and prior austenite grain boundaries, resulting from tempering at 280°C, were similar for the two austenitizing treatments. The discrete precipitation of cementite at prior austenite grain boundaries was observed in both cases. The factors that affect the detection of tempered martensite embrittlement in room temperature tests were discussed. The observed embrittlement in the 1200°C austenitized specimens (after tempering at 280°C and 350°C) was believed to be associated with the large prior austenite grains, which possibly enhance the detection (or severity) of tempered martensite embrittlement in room temperature tests by raising the fracture toughness transition temperature.

INTRODUCTION

The most difficult problem encountered in designing high-strength alloys is the general trend of decreasing toughness with increasing strength. Achieving high strengths has been relatively easy, but a concomitant increase in toughness to resist brittle fracture has proved much more difficult. The high-strength low-alloy steels currently in use were developed decades ago by trial and error methods. They all have a low fracture toughness at high yield strength levels, i.e., above 200,000 psi.

It is well known that the fracture toughness of high-strength steels is strongly dependent on their microstructures. When undesirable microstructural features are present, it is sometimes possible to eliminate them through either an alternative heat treatment or suitable changes in chemical composition. In recent studies at the University of California on a secondary hardening steel of 5 Mo-0.3 C, it was found that undesirable microstructural features could be eliminated by using a much higher austenitizing temperature than is employed in conventional heat treating. As a result, a large increase in fracture toughness was obtained.[1]

The conventional heat treatment used in commercial practice for quenched and tempered low-alloy steels is to austenitize at the lower end of the austenite temperature range (850-900°C) to minimize the austenite grain size. This heat treatment results in an alloy with low toughness at high yield strength levels (above 200,000 psi). The objectives of this investigation were (1) to identify the undesirable microstructural features that cause poor toughness at high strength

levels when conventional heat treatment is employed, and (2) to explore new heat treatments in an effort to obtain desirable microstructures that would provide improved toughness while maintaining the same high strength levels. An aircraft quality commercial low alloy steel AISI 4340 was used for this investigation.

EXPERIMENTAL PROCEDURE

The AISI 4340 steel used in this investigation was received in a fully annealed condition. It had the following chemical composition in wt%: 0.40 carbon, 0.80 manganese, 0.72 chromium, 1.65 nickel, 0.24 molybdenum, 0.24 silicon, 0.19 copper, 0.01 sulphur and 0.004 phosphorous. Two austenitizing treatments were used throughout. The conventional heat treatment, commonly used in commercial practice consisted of austenitizing at 870°C for 1 hr. The new heat treatment consisted of austenitizing at a much higher temperature, 1200°C, for 1 hr followed by cooling to 870°C and holding for half an hour. All specimens were quenched into room temperature oil. Tempering was carried out for 1 hr at various temperatures. Both heat treatments were conducted in an argon atmosphere, and salt baths were used for tempering.

Tensile properties were measured with round specimens, 0.357 in diameter and 1.4 in gauge length. These specimens were ground from the blanks that had been previously heat treated. The plane strain fracture toughness was determined using the ASTM specified[2] compact tension testing specimens. All fracture toughness specimens were machined from 5/8 in. thick bar stock to final dimensions except for the thickness and an 0.008 in. thick slot. After heat treating, 0.010 in. was ground off each side, and an 0.008 in. thick slot was machined to act as a notch for introducing a fatigue crack. A 300 kip M.T.S. machine was used for tensile testing and fatigue precracking of the compact tension specimen, and a 5,000 kg capacity Instron was used for fracture toughness testing, which was conducted in accordance with ASTM standards.[2] Both tensile and fracture toughness tests were performed at room temperature

at a cross heat speed of 0.04 in./min; all specimens were tested in the longitudinal direction. The stress intensities were determined from the collocation solution given by Srawley and Gross.[3]

Thin foils for transmission electron microscopy examination were obtained directly from the fracture toughness specimen to insure that there would be no ambiguity in correlating microstructure with fracture toughness. The 0.020 in. thick samples were first mechanically sectioned with extreme care in flood cooling from the fracture toughness specimen. Next, they were chemically thinned down to 0.005 in. thick in a mixture of hydrofluoric acid and hydrogen peroxide. Foils were then obtained from these samples by electropolishing them in chromic-acetic electrolyte, using the window technique. Foils were then examined in a Siemens Elmiskop IA electron microscope, operated at 100 kV.

The fracture surface of the fracture toughness specimen was examined in a Jeolco JSM-U3 scanning electron microscope with a secondary emission operated at 25 kV.

RESULTS

Mechanical Properties

The mechanical properties of the specimens austenitized at both 870°C and 1200°C as a function of tempering temperature are presented in Fig. 1. The yield and tensile strengths were substantially identical in all tempered conditions. However, the plane strain fracture toughness, K_{IC}, in the as-quenched condition was greatly improved when the 1200°C austenitizing temperature was used. An approximate 80% increase in fracture toughness was obtained for as-quenched specimens by raising the austenitizing temperature from 870°C to 1200°C.

The plane strain fracture toughness vs tempering temperature was also affected by the change of austenitizing temperature. For the specimen austenitized at 870°C, the plane strain fracture toughness remained relatively constant after tempering at 200°C and 280°C and increased at higher tempering temperatures. There was no clear evidence of embrittlement after tempering at 200°C to 350°C. The embrittlement is generally manifested by a toughness drop in a plot of toughness vs tempering temperature. However, for the specimen austenitized at 1200°C, the plane strain fracture toughness increased after tempering at 200°C from that of the as-quenched condition and decreased abruptly after tempering at 280°C and 350°C. The embrittlement, which is generally referred to as tempered martensite embrittlement, was observed after tempering at 280°C and 350°C.

The values of the plane strain fracture toughness vs tempering temperature from 200°C to 350°C for the specimen austenitized at 870°C generally agreed well with the published data for this steel.[4,5]

However, no data are available in the literature on the plane strain fracture toughness as a function of tempering temperature for this steel or steels with similar composition austenitized at a much higher temperature.

Fractography

The marked difference in the mechanical behavior of the steel with two different austenitizing treatments required a detailed examination of the fracture surface. The mode of fracture for the as-quenched specimen changed from a mixture of dimpled rupture and quasi-cleavage to precomantly dimpled rupture when austenitizing temperature was changed from 870°C to 1200°C, Fig. 2.

For the specimen austenitized at 1200°C, the fracture surface when tempered at 200°C is similar to that of the as-quenched specimen except featuring much deeper dimples, indicating more plastic deformation before fracture. However, the mode of fracture becomes intergranular fracture (with respect to austenite grains) when tempered at 280°C and 350°C, Fig. 3(b), where an embrittlement occurs, as shown in Fig. 1. In contrast, for the specimen austenitized at 870°C, the topographical feature in the fracture surface when tempered at 280°C is composed of a mixture of dimples and quasi-cleavage facets. This feature is similar to that in the as-quenched specimens with the same austenitizing treatment, Fig. 3(a).

As-Quenched Structure

The increase in austenitizing temperature from 870°C to 1200°C resulted in an increase in austenite grain size from ASTM 7-8 to ASTM 0-1.

Extensive examination by optical microscopy, replica techniques, and thin foil electron microscopy failed to reveal the presence of austenite decomposition products, such as pro-eutectoid ferrite and upper bainite, with the exception of a small amount of lower bainite as observed by transmission electron microscopy in the as-quenched specimens with both austenitizing treatments. Oil quenching, as practiced throughout this investigation, after austenitization at either 870°C or 1200°C resulted in mainly a martensitic structure in this steel.

Two types of martensite morphology were observed in the as-quenched structure austenitized at either 870°C or 1200°C. The large martensite plates, which form as individual plates, some of which were marked as P in Fig. 4(a,b,c), are characterized as the plate martensite.[6] The second type of martensite morphology observed is characterized as lath martensite,[6-8] in which laths are generally aligned parallel to one another in groups that are termed packets, Fig. 4(b,c,d).

Substructure of Martensite

The substructure of both plate and lath martensites in the steel austenitized at both temperatures was studied extensively by transmission electron microscopy.

Lath Martensite. It was observed that changing the austenitizing temperature did not affect the martensite lath size significantly, Fig. 4(b,d). The martensite laths, which are generally separated from one another by low angle boundaries within the packet or bundle, contain

a high density of tangled dislocations. Occasionally, the lath contains a few internal twins, Fig. 4(b,d). The amount of these twins in martensite laths, however, remains small and is relatively unchanged wither the steel is austenitized at 870°C or 1200°C.

Plate Martensite. The large martensite plates observed in the steel austenitized at 870°C consisted of two different types of substructure. Some plates contain mainly dislocations, Fig. 4(b), while many others contain extensive fine transformation twins in addition to dislocations, Fig. 5. The observation of untwinned plates was not due to the orientation effect of the plate with respect to the electron beams, since extensive foil tilting was done in the examination of each plate. Furthermore, it was found that the untwinned plates contained numerous fine carbides due to autotempering, whereas the twinned plates did not. This may indicate that the twinned plates were formed at lower temperatures. The twins in the martensite plate were identified by the electron diffraction pattern and dark field imaging of twin spots, and their twin planes determined as $\{112\}_M$, Fig. 6. These twinned martensite plates, however, were eliminated when austenitized at a much higher temperature, i.e., 1200°C. The large martensite plates observed when austenitized at 1200°C contain numerous fine cross-hatched ε carbides due to autotempering, with a definite lack of twinning, Fig. 7. The ε carbide in a cross-hatched arrangement is similar to that observed by other investigators.[9] The occurrence of autotempering in the as-quenched specimens will be discussed later.

The kinetics study of 4340 steel[10] in the authors' laboratory has shown that the increase in austenitizing temperature (also in austenite

grain size) from 870°C to 1200°C resulted in a concomitant increase in M_s temperature from 290°C to 327°C with M_f temperature remaining relatively unchanged. Increasing M_s temperature with increasing grain size was also observed in a Fe-30% Ni alloy.[11]

Kelly and Nutting[12] related the increasing amount of twinning to the lowering of M_s temperature. However, a recent investigation[13] on Fe-Ni-Co-C steels has suggested that M_s temperature is not a sufficient indication of the extent of twinning in martensite. It is doubtful that the conclusion of this investigation[13] can be generalized since in this investigation steels with a wide range of different compositions were used for comparison. It is believed that for the same steel there is a definite correlation between M_s temperature and the extent of twinning in martensite plates.

Retained Austenite

Another prominent change in microstructure when austenitizing temperature was increased from 870°C to 1200°C was the concomitant large increase in retained austenite films surrounding martensite laths. There was, however, virtually no retained austenite in the as-quenched specimen austenitized at 870°C. Figure 8 shows a typical area containing films of retained austenite that can be resolved by dark-field imaging technique. The dark-field image, Fig. 8(b), showing the reversal contrast of retained austenite films was formed from a (200) austenite reflection beam. Figure 8(c) is a typical selected area diffraction pattern from the area containing retained austenite. Both martensite and austenite diffraction patterns were indexed in Fig. 8(d).

The retained austenite, approximately 100 to 200Å thick, exhibits the Kurdjumov-Sachs orientation relationship with respect to martensite, i.e., $\langle 111 \rangle_M \parallel \langle 110 \rangle_\gamma$, Fig. 8(c), which is in agreement with the results of earlier workers.[12] A previous investigation[12] has shown that prior plastic deformation before quenching tends to stabilize austenite, which becomes more difficult to transform to martensite. It has been observed that the plastic deformation is produced in the surrounding austenite when martensite forms.[12,13] Kelly and Nutting[12] observed that the disslocation density in the surrounding austenite can be as high as 10^{11} or $10^{12}/cm^2$ when martensite forms. The increasing stability of the remaining austenite when the steel is partially transformed to martensite appears to be related to the deformation that accompanies the formation of martensite. It appears that increasing the amount of retained austenite films with increasing austenitizing temperature that accompanies an increase in austenite grain size is the result of the increasing stability of austenite. It is believed that the deformation in the surrounding austenite accompanying the formation of martensite may extend far beyond the vicinity of martensite. Thus, the increasing stability of austenite is likely due to increased deformation resulting from the formation of more martenite laths within the austenite grain because of a much larger austenite grain size when austenitized at 1200°C. It is not, however, due to the solution of alloying impurities in the austenite which lowers both M_s and M_f temperatures when the austenitizing temperature is raised so as to stabilize the austenite, because M_s was observed to increase when the austenitizing temperature was increased from 870°C to 1200°C with the M_f temperature relatively unchanged.[10]

It was also found that the retained austenite did not decompose, as determined by transmission electron microscopy, when the specimen was refrigerated in liquid nitrogen immediately after quenching. This indicates the retained austenite is so highly dislocated during the successive formation of martensite laths that it remains stable even at liquid nitrogen temperature. The overall percentage of retained austenite was not detected by the X-ray method using copper radiation. This could mean either that the total amount of retained austenite is below the limit of detection by the X-ray method employed (approximately 3%) or that the amount of retained austenite, which may well be above the limit of detection by X-ray method, is too highly deformed to allow such detection.

Autotempering

Autotempering was observed in as-quenched specimens austenitized at either 870°C or 1200°C. Two types of carbides, namely cementite and ε carbide, formed as a result of autotempering. No lath boundary carbides were observed. Cementites formed as a fine particles within martensite laths. A typical micrograph illustrating autotempered martensite containing cementite is shown in Fig. 9 for the 1200°C austenitizing treatment. A similar structure was also obtained for the 870°C treatment. The ε carbide that formed in a cross-hatched pattern in autotempered martensite was identified by trace analysis of its habit planes and by dark field imaging. Micrographs illustrating the morphology of ε carbide are shown in Fig. 10 for both austenitizing treatments. The present investigation showed the ε carbide formed on $\{100\}_\alpha$ planes and along $\langle 100\rangle_\alpha$ directions, in agreement with the findings of other investigators.[9,15]

Detecting autotempering in the as-quenched specimens required a simultaneous examination of both bright and dark field images, as well as selected area electron diffraction examination, all coupled with extensive foil tilting during scanning of the foil. Thus, obtaining quantitative estimates of the extent of autotempering resulting from the two different austenitizing treatments was extremely difficult.

Structure of Tempered Martensite

Tempering at 200°C for the specimens austenitized at either 870°C or 1200°C produced a uniform dispersion of ε carbides within martensite laths and plates. No lath boundary carbides were observed. The retained austenite in as-quenched specimens did not decompose after tempering at 200°C. However, it decomposed at 280°C and 350°C.

In specimens austenitized both at 870°C and 1200°C cementite was the predominant carbide formed during tempering at 280°C although in a very few regions ε carbides was also detected. Cementite precipitation occurred both at lath boundaries and within laths and plates as illustrated in Fig. 11. In addition, the precipitation of cementite as discrete platelets at prior austenite grain boundaries was also observed as shown in Figs. 12 and 13. Grain boundary precipitation of carbides did not result in continuous carbide networks. The distribution and morphology of cementite at both lath boundaries and prior austenite grain boundaries were not significantly different for the two austenitizing treatments.

DISCUSSION

Factors Contributing to the Improvement of Fracture Toughness

It is clearly shown that a large improvement in fracture toughness in 4340 steel was obtained in as-quenched and low-temperature tempered conditions by using a much higher austenitizing temperature (1200°C instead of 870°C). This improvement in fracture toughness was accompanied by a change of fracture mode from a mixture of dimpled rupture and quasi-cleavage to predomonantly dimpled rupture when the austenitizing temperature was changed from 870°C to 1200°C.

The increase in fracture toughness with increasing austenitizing temperature in a 5 Mo-0.3 C secondary hardening steel was attributed to the elimination or at least minimization of undissolved carbides.[16] For 4340 steel, the 870°C austenitizing temperature was high enough to produce a structure with very few undissolved carbides. For steels with hardenability lower than 4340, such as 4130 and 4140, it has been found that increasing fracture toughness with increasing austenitizing temperature was a result of minimizing the undesirable austenite decomposition products, such as pro-eutectoid ferrite and upper bainite, formed during quenching.[16,17] However, results of this investigation show that oil quenching of a 5/8 in. thick 4340 steel after austenitizing at either temperature produced mainly a martensitic structure.

The as-quenched structure obtained from both austenitizing treatments consists of both autotempered and untempered martensites. It is known that the toughness of the as-quenched martensite is improved with the occurrence of autotempering. The difference, if any, in the extent of autotempering in the as-quenched structures been two different austenitizing

treatments could not be quantitatively determined from the present investigation. However, the similarity in ultimate tensile strength levels in as-quenched conditions after both austenitizing treatments suggests that the difference was not large enough to contribute to the observed large difference in fracture toughness between two austenitizing treatments.

The martensite morphology in as-quenched structures following both austenitizing treatments was characterized by laths and plates. For both austenitizing treatments, the martensite laths are dislocated, with occasionally a few internal twins. However, many martensite plates contain extensive fine internal twins when austenitized at 870°C. These twinned martensite plates were eliminated when the steel was austenitized at 1200°C. It was concluded that the elimination of twinned martensite plates was at least partly responsible for the observed increase in fracture toughness of the specimens austenitized at 1200°C.

The loss of toughness due to the presence of extensive twinning has also been reported by other investigators,[13,18] who compared the toughness of twinned martensite and lower bainite (untwinned) and of twinned martensite and dislocated martensite. The exact role of twinning on toughness is not yet clear. Kelly and Nutting[12] suggested that the available slip system would be reduced by a factor of four by the presence of twins, since the operative slip system must be such that both the slip plane and the slip direction are common to both the twin and the matrix. Krauss, et al.[19] and Bevis, et al.[20] indicated that the martensite with the presence of twinning is more likely to

deform by mechanical twinning than slip. Cracks induced by twins in metals have been observed by Gilbert, et al.[21]

Another prominent microstructural change accompanying the change of austenitizing temperature from 870°C to 1200°C was a large increase in the amount of retained austenite films. Austenite is known to be a tough phase that can effectively arrest the propagation of cracks. Increases in toughness with increasing retained austenite content in steels have also been observed before.[22] It has been suggested that for improving toughness, the distribution of the retained austenite phase may be more important than the total amount of the phase. The austenite phase observed in the steel austenitized at 1200°C is in the form of films surrounding martinsite laths. The austenite can then relax the stress concentration to delay the formation of microcracks and also can effectively arrest further propagation once microcracks develop. This can result in considerable enhancement of fracture toughness.

Tempered Martensite Embrittlement

For the specimen austenitized at the conventional 870°C with an austenite grain size ASTM 7-8, the room temperature plane strain fracture toughness measurements failed to reveal tempered martensite embrittlement after tempering at 200 to 350°C. The fracture mode of all tempered specimens was observed to be transgranular with respect to prior austenite grains, and to consist of a mixture of dimpled rupture and quasi-cleavage.

However, for the specimen austenitized at 1200°C with an austenite grain size ASTM 0-1, the embrittlement was observed after tempering at

280 and 350°C. The fracture mode of the embrittled specimen was intergranular fracture along prior austenite grain boundaries, while that of unembrittled specimens (as-quenched condition or tempered at 200°C) was dimpled rupture.

The microstructural observation showed that embrittlement occurred when cementite was the predomnant precipitate phase formed during tempering at 280 and 350°C. However, it failed to explain the different fracture behavior between the observed embrittlement in the 1200°C austenitized course grain specimen and the apparent absence of embrittlement in the 870°C austenitized fine grain specimen after tempering at the embrittling temperature range, since both the distribution and morphology of cementite platelets at both lath boundaries and prior austenite grain boundaries were found to be similar for the two austenitizing treatments. It is thus believed that the difference in fracture behavior between the 1200°C austenitized coarse grain specimen and the 870°C austenitized fine grain specimen after tempering at 280°C and 350°C might be due to other factors, to be subsequently discussed.

Tempered martensite embrittlement has been previously reported by a number of investigators[23-25] in room temperature Charpy impact tests. With recent success in fracture toughness theory and testing, considerable data have been produced on the effect of tempering temperature on fracture toughness in AISI 4340 or the steels with similar composition.[4,5,26-29] All specimens in these investigations were austenitized at around 870°C, which resulted in fine austenite grains, and were tested at room temperature. All these data in a plot of plane strain fracture toughness vs tempering temperature showed no evidence of tempered

martensite embrittlement. Some data showed the fracture toughness increases smoothly with increasing temperature, while others showed the fracture toughness remains relatively constant in the 200°C to 300°C range and increases rapidly at higher tempering temperature. The present investigation showed similar results with no apparent embrittlement when specimens were austenitized at 870°C to result in fine austenite grains. Nevertheless, embrittlement was observed when specimens were austenitized at 1200°C to result in coarse austenite grains.

Ronald[31] recently investigated tempered martensite embrittlement of AISI 4340 by using V-notched and fatigue-precracked Charpy specimens of various sizes tested in impact and slow bend modes. The specimens were austenitized at around 850°C and were tested at room temperature. In a plot of energy per unit area absorbed in breaking the specimen vs tempering temperature, he found that detection of the embrittlement depends on the type and size of the specimen and on the type of testing, i.e., impact or slow bend. In impact testing, the embrittlement was always observed with varied specimen thickness whether the specimen was V-notched or precracked. In slow bend testing, the embrittlement was always observed in V-notched specimens with varied thickness from 0.030 to 0.394 in.; and while the precracked specimens were used, the embrittlement was observed only in thin specimens from 0.030 to 0.050 in. and was not in thick specimens from 0.075 to 0.394 in.

Kula, et al.,[5] while observing tempered martensite embrittlement on AISI 4340 in room temperature Charpy impact tests, found no evidence of embrittlement in room temperature K_{IC} tests. However, he observed a slight embrittlement when K_{IC} tests were conducted at -50°F.

The above discussion indicates that the detection of tempered martensite embrittlement depends on many parameters including the type and size of the specimen, loading rate (static or dynamic), and testing temperature. Varying some of these parameters, for example, increasing the loading rate from static to dynamic or decreasing testing temperature, could enhance the detection of tempered martensite embrittlement.

There is little information on transition temperature for fracture toughness values in low-alloy high-strength steels. Steigerwald[32] observed that the plane strain fracture toughness continued to decrease relatively sharply as the testing temperature decreased from room temperature to -100°F for AISI 4340 and 4140 austenitized at 850°C and then tempered at either 260°C or 472°C. Increasing grain size is known to result in an increase in impact transition temperature. It is reasonable to expect that increasing grain size may also result in an increase in fracture toughness transition temperature. The likelihood of detecting tempered martensite embrittlement is enhanced when the testing temperature is at or below the fracture toughness transition temperature. It was believed that the observed tempered martensite embrittlement in the 1200°C austenitized coarse grain specimens of the present investigation was due to increased prior austenite grain size, which possibly raised the fracture toughness transition temperature to above room temperature.

Although the mechanism of tempered martensite embrittlement cannot be determined in this investigation, some general comments can be made. Tempered martensite embrittlement has been the subject of many investigations, but the embrittlement mechanism has not yet been determined.

Previous investigators[25,32,33] have, however, generally agreed that the occurrence of embrittlement is associated with the precipitation of cementite platelets. It was further demonstrated by Alstetter, et al.[34] that an increase in silicon content raised the temperature at which cementite precipitation began and also raised the tempering temperature at which embrittlement occurred. The present microstructural observation substantiated that the embrittlement occurred when cementite was the predominant carbide phase. In addition to the precipitation of cementite both within the laths and at lath boundaries, the discrete precipitation of cementite platelets was observed at prior austenite grain boundaries. The fracture mode of the embrittled steel was intergranular fracture along prior austenite grain boundaries. In a similar investigation on AISI 4130,[17] which also exhibited tempered martensite embrittlement with an intergranular fracture in the 1200°C austenitized specimen tempered at 280°C, discrete cementite platelets were observed at prior austenite grain boundaries. It is not clear whether the discrete grain boundary carbide alone under appropriate conditions, i.e., testing temperature, loading rate, prior austenite grain size, etc, could induce intergranular fracture thus causing embrittlement. Recent work by Capus, et al.[35] has shown that the presence of certain impurity elements has a significant influence on tempered martensite embrittlement. An embrittlement model proposed by Kula, et al.[5] suggested that when the cementite at prior austenite grain boundaries grows during tempering, certain impurity elements, such as phosphorous, which might be more soluble in ferrite than in cementite, will diffuse out of cementite into the surrounding ferrite. This results in a

segregated film of impurities at the interface between ferrite and cementite. These impurities might lower the interfacial energy to provide a weak interface for fracture.

SUMMARY AND CONCLUSIONS

The room temperature plane strain fracture toughness of AISI 4340 was greatly improved without loss in strength levels in both the as-quenched and low-temperature tempered conditions when the austenitizing temperature was raised from the conventional practiced 870°C to 1200°C. This improvement in fracture toughness with increasing austenitizing temperature is attributed to (a) the elimination or at least minimization of twinned martensite plates and (b) the large increase in the amount of retained austenite films which surround martensite laths.

When the specimens were austenitized at 870°C with an austenite grain size ASTM 7-8, no evidence of tempered martensite embrittlement was observed in the room temperature plane strain fracture toughness measurements. This agrees with previous investigations by other workers. However, embrittlement was observed after tempering at 280°C and 350°C when the specimens were austenitized at 1200°C with an austenite grain size ASTM 0-1. Both the distribution and morphology of cementite platelets at both lath boundaries and prior austenite grain boundaries were found to be similar between the two different austenitized specimens tempered at 280°C. The discrete precipitation of cementite at prior austenite grain boundaries was observed in both cases. The microstructural observations failed to reveal different fracture behavior between the 1200°C and 870°C austenitized specimens after tempering at 280°C.

From a study of the results reported in the literature and the evidence obtained in the present investigation, it was concluded that the detection of tempered martensite embrittlement was dependent on many parameters such as loading rate (static or dynamic), testing temperature, prior

austenite grain size, and specimen geometry. The observed embrittlement in the 1200°C austenitized specimen after tempering at 280°C and 350°C was believed to be associated with the large austenite grains, which possibly enhance the detection (or severity) of tempered martensite embrittlement in room temperature tests by raising the fracture toughness transition temperature.

ACKNOWLEDGEMENTS

The authors gratefully acknowledge the valuable help of Dr. Dilip Bandarkar and Dr. M. Yokota for their critical review of the manuscript.

This research was performed partially under the auspices of the U. S. Atomic Energy Commission through the Inorganic Materials Research Division of the Lawrence Berkeley Laboratory, Contrast No. W-7405-eng-48 and partially under the auspices of the Army Materials and Mechanics Research Center, Watertown, MA, Contract No. DAAG46-73-C-0120.

REFERENCES

1. V. F. Zackay, E. R. Parker, R. D. Goolsby and W. E. Wood: Nature Phys. Sci., 1972, vol. 236(68), p. 108.
2. Annual Book of ASTM Standards, E 399-72, (American Society of Testing and Materials), Philadelphia, p. 960, 1973.
3. J. E. Srawley and B. Gross: Mater. Res. Stand., 1967, vol. 7, p. 155.
4. A. J. Baker, F. J. Lauta and R. P. Wei: ASTM STP 370, American Society for Testing and Materials, Philadelphia, 1963, p. 3.
5. E. B. Kula and A. A. Anctil: J. of Materials, 1969, vol. 4(4), p. 817.
6. G. Krauss and A. R. Marder: Met. Trans., 1971, vol. 2, p. 2343.
7. J. M. Marder and A. R. Marder: Trans. ASTM, 1969, vol. 62, p. 1.
8. W. S. Owen, E. A. Wilson and T. Bell: High Strength Materials, V. F. Zackay, ed., John Wiley and Sons, New York, 1965, p. 167.
9. E. Tekin and P. M. Kelly: Precipitation from Iron-Base Alloys, AIME, New York, 1965, p. 173.
10. B. Babu: unpublished results, University of California, Berkeley, California.
11. M. Cohen, E. S. Machlin and V. G. Paranjpe: Thermodynamics of Physical Metallurgy, ASM, Metals Park, Ohio, 1949.
12. P. M. Kelly and J. Nutting: J. of the Iron and Steel Institute, 1961, vol. 197, p. 199.
13. S. K. Das and G. Thomas: Trans. ASM, 1969, vol. 62, p. 659.
14. B. Edmondson and T. Ko: Acta Met., 1954, vol. 2, p. 235.
15. M. G. H. Wells: Acta Met., 1964, vol. 12, p. 389.

16. V. F. Zackay, E. R. Parker and W. E. Wood: Microstructure and Design of Alloys, Institute of Metals, London, 1973, p. 175.

17. G. Y. Lai, W. E. Wood, E. R. Parker and V. F. Zackay: unpublished results.

18. Der-Hung Huang and G. Thomas: Met. Trans., 1971, vol. 2, p. 1587.

19. C. Krauss and W. Pitsch: Acta Met., 1964, vol. 12, p. 278.

20. M. Bevis, P. C. Rowlands and A. F. Acton: Trans. AIME, 1968, vol. 242, p. 1555.

21. A. Gilbert, G. T. Hahn, C. N. Reid and B. A. Wilcox: Acta Met. 1964, vol. 12, p. 754.

22. D. Webster: Trans. ASM. 1968, vol. 61, p. 816.

23. M. A. Grossmann: Trans. AIME, 1946, vol. 167, p. 39.

24. R. L. Rickett and J. M. Hodge: Proceedings, ASTM, 1951, vol. 51, p. 931.

25. L. J. Klingler, W. J. Barnett, R. P. Frohmberg and A. R. Troiano, Trans. ASM, 1954, vol. 46, p. 1557.

26. W. A. Backofen and M. L. Ebner: WAL TR 310.24/5-4, 1963, Army Materials and Mechanics Research Center.

27. M. F. Amateau and E. A. Steigerwald: Contract No. 64-0186C, 1965. U. S. Bureau of Naval Weapons.

28. F. J. Lauta and E. A. Steigerwald: AFML-TR-65-31, 1965, Air Force Materials Laboratory.

29. W. G. Ferguson and M. N. Sargisson: Engineering Fracture Mechanics, 1973, vol. 5, p. 499.

30. T. M. F. Ronald: Met. Trans., Vol. 1, Sept. 1960, p. 2583.

31. E. A. Steigerwald: Engineering Fracture Mechanics, 1969, vol. 1, p. 473.

32. B. S. Lement, B. L. Averbach and M. Cohen: Trans. ASM, 1954, vol. 46, p. 851.

33. B. R. Banerjee: J. Iron and Steel Institute, 1965, vol. 203, p. 166.

34. C. J. Alstetter, M. Cohen and B. L. Averbach: Trans. ASM, 1962, vol. 55, p. 287.

35. J. M. Capus and G. Mayer: Metallurgica, 1960, vol. 62, p. 133.

FIGURE CAPTIONS

Fig. 1. Effect of austenitizing and tempering temperatures on strength and fracture toughness of AISI 4340 steel.

Fig. 2. Scanning electron micrographs of the fracture surface of as-quenched specimens austenitized at (a) 870°C showing dimples and quasi-cleavage facets and (b) 1200°C showing predominantly dimples.

Fig. 3. Scanning electron micrographs of the fracture surface of the specimens tempered at 280°C after austenitizing at (a) 870°C showing a mixture of dimples and quasi-cleavage facets and (b) 1200°C showing predominantly intergranular fracture.

Fig. 4. As-quenched structure of the specimen austenitized at (a,b) 870°C and (c,d) 1200°C. (a) Optical micrograph, and (b) transmission electron micrograph, showing a mixture of martensite laths and plates. (c) Optical micrograph showing both martensite plates at prior austenite grain boundaries and martensite laths within prior austenite grains, and (d) transmission electron micrograph showing a typical area of martensite laths. Some martensite plates are marked as P and the internal twins in martensite laths are indicated by the small arrow.

Fig. 5. Transmission electron micrographs of martensite plates in the as-quenched specimen austenitized at 870°C, showing extensive fine transformation twins.

Fig. 6. Transmission electron micrographs of a twinned martensite plate in the as-quenched specimen austenitized at 870°C. (a) Bright field image showing the $\{112\}_M$ transformation twins and the electron diffraction pattern showing both the martensite and twin diffraction patterns, (b) dark field image of twin spot (indicated by the arrow) showing the reversal contrast of the twins.

Fig. 7. Transmission electron micrograph of the martensite plate (marked as P) in the as-quenched specimen austenitized at 1200°C showing the absence of twinning. The plates contain numerous cross-hatched ε carbides formed during quenching.

Fig. 8. Transmission electron micrographs of the as-quenched specimen austenitized at 1200°C showing extensive amounts of retained austenite films surrounding martensite laths: (a) bright field image, (b) dark field image of austenite reflection showing the reversal contrast of retained austenite films (c) selected area diffraction pattern, and (d) schematic sketch of the selected area diffraction pattern with austenite (γ) and martensite (M) reflections indexed.

Fig. 9. Typical autotempered martensite associated with fine cementites in the as-quenched specimen austenitized at 1200°C: (a) bright field image, (b) dark field image of cementite reflection. These micrographs are also representative of autotempered martensite in the specimen austenitized at 870°C.

Fig. 10. Typical autotempered martensite associated with ε carbides which form on $\{100\}_\alpha$ planes and along $\langle 100\rangle_\alpha$ directions in the

as-quenched specimens austenitized at (a) 870°C and (b) 1200°C.

Fig. 11. Dark field micrographs formed from a cementite reflection showing the precipitation of cementites both at lath boundaries and within the laths in the specimens tempered at 280°C after austenitizing at (a) 870°C and (b) 1200°C.

Fig. 12. Transmission electron micrograph of the specimen tempered at 280°C after austenitizing at 870°C, showing discrete precipitation of cementite platelets at prior austenite grain boundaries (marked GB).

Fig. 13. Transmission electron micrographs of the specimen tempered at 280°C after austenitizing at 1200°C showing discrete precipitation of cementite platelets at prior austenite grain boundaries (marked GB): (a) bright field image, (b) dark field image of cementite reflection.

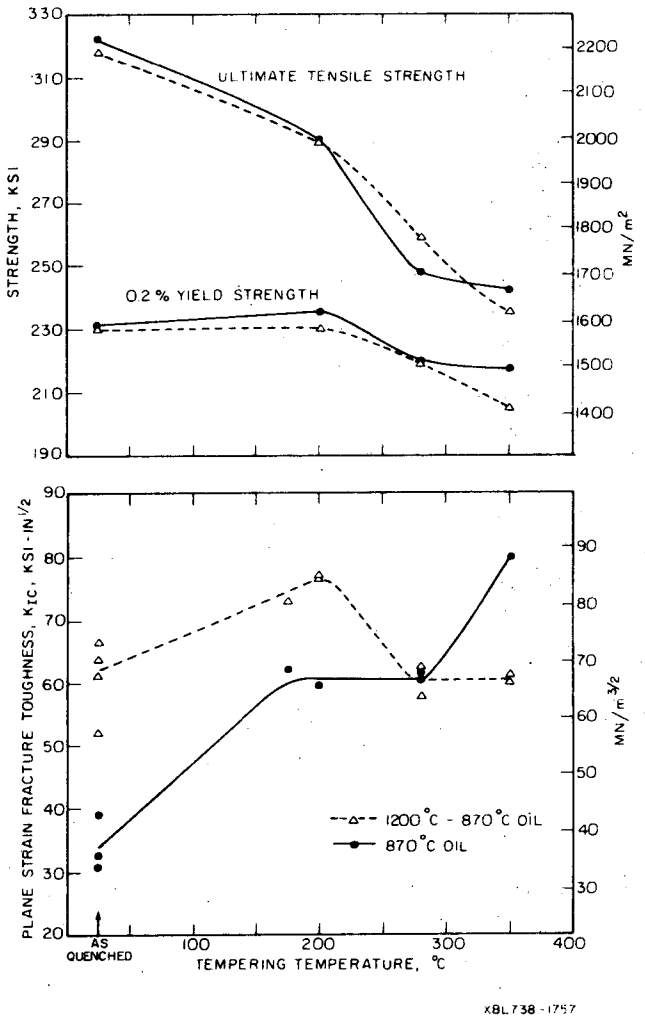
ULTIMATE TENSILE STRENGTH
0.2% YIELD STRENGTH
STRENGTH, KSI
MN/m²
PLANE STRAIN FRACTURE TOUGHNESS, K1C, KSI-IN1/2
MN/m3/2
1200°C - 870°C OIL
870°C OIL
AS QUENCHED
TEMPERING TEMPERATURE, °C
XBL738-1757

Fig. 1

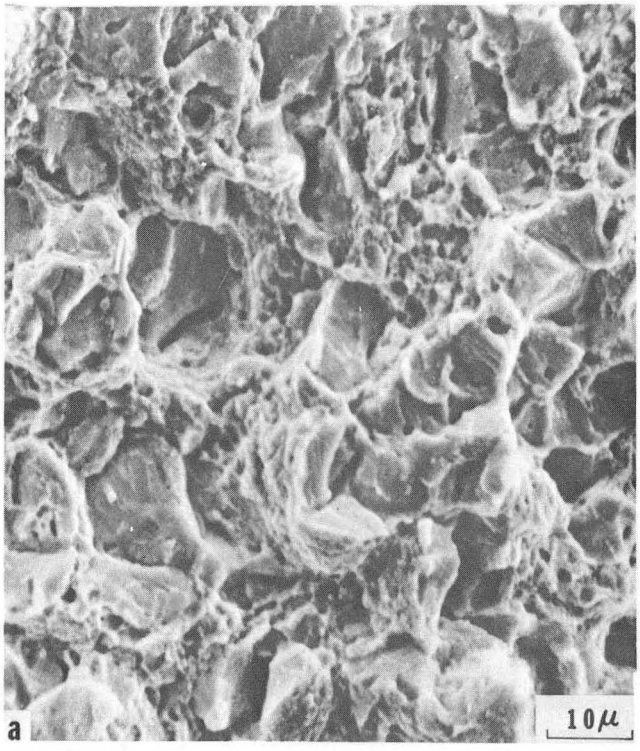

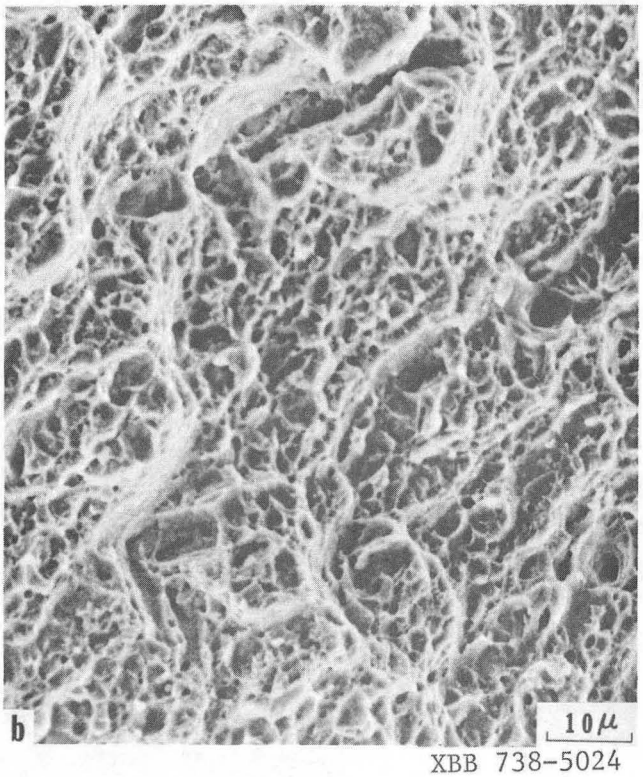

XBB 738-5024

Fig. 2

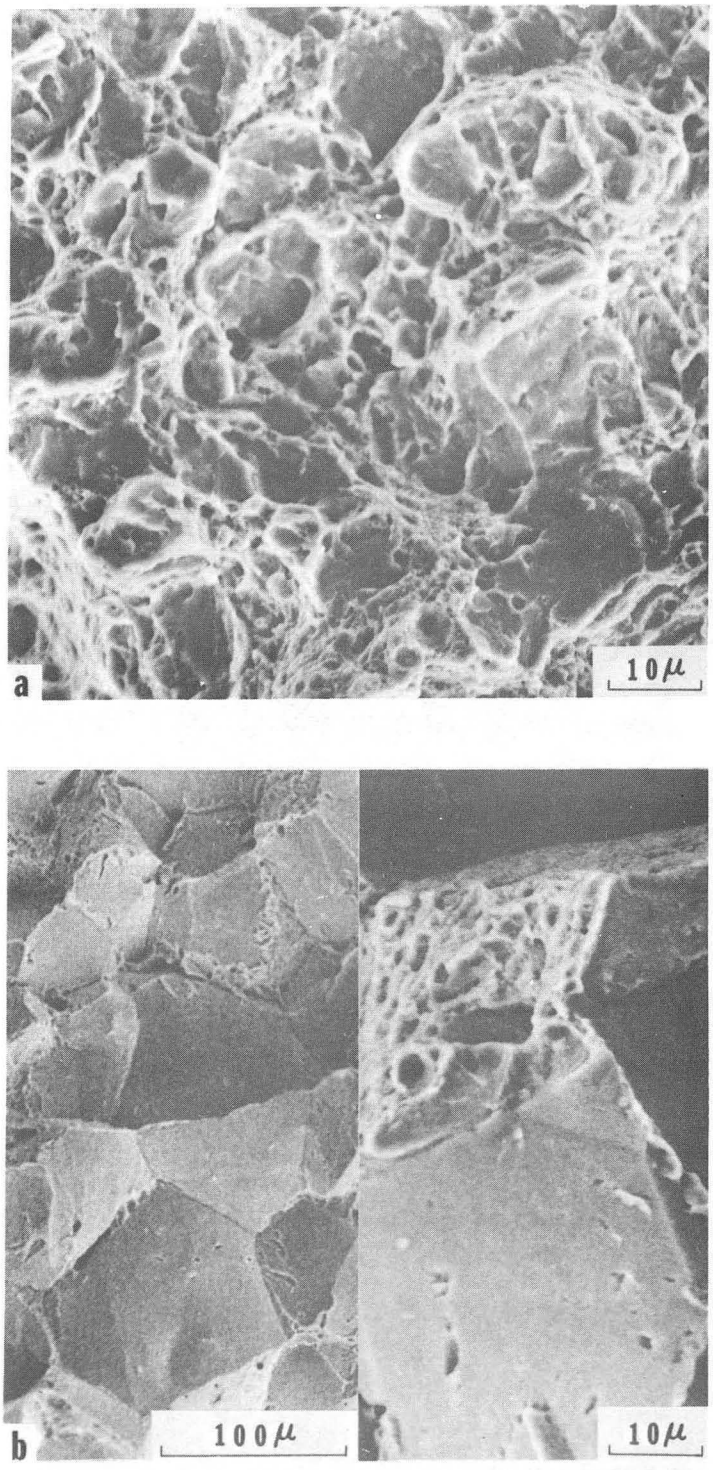

XBB 738-5019

Fig. 3

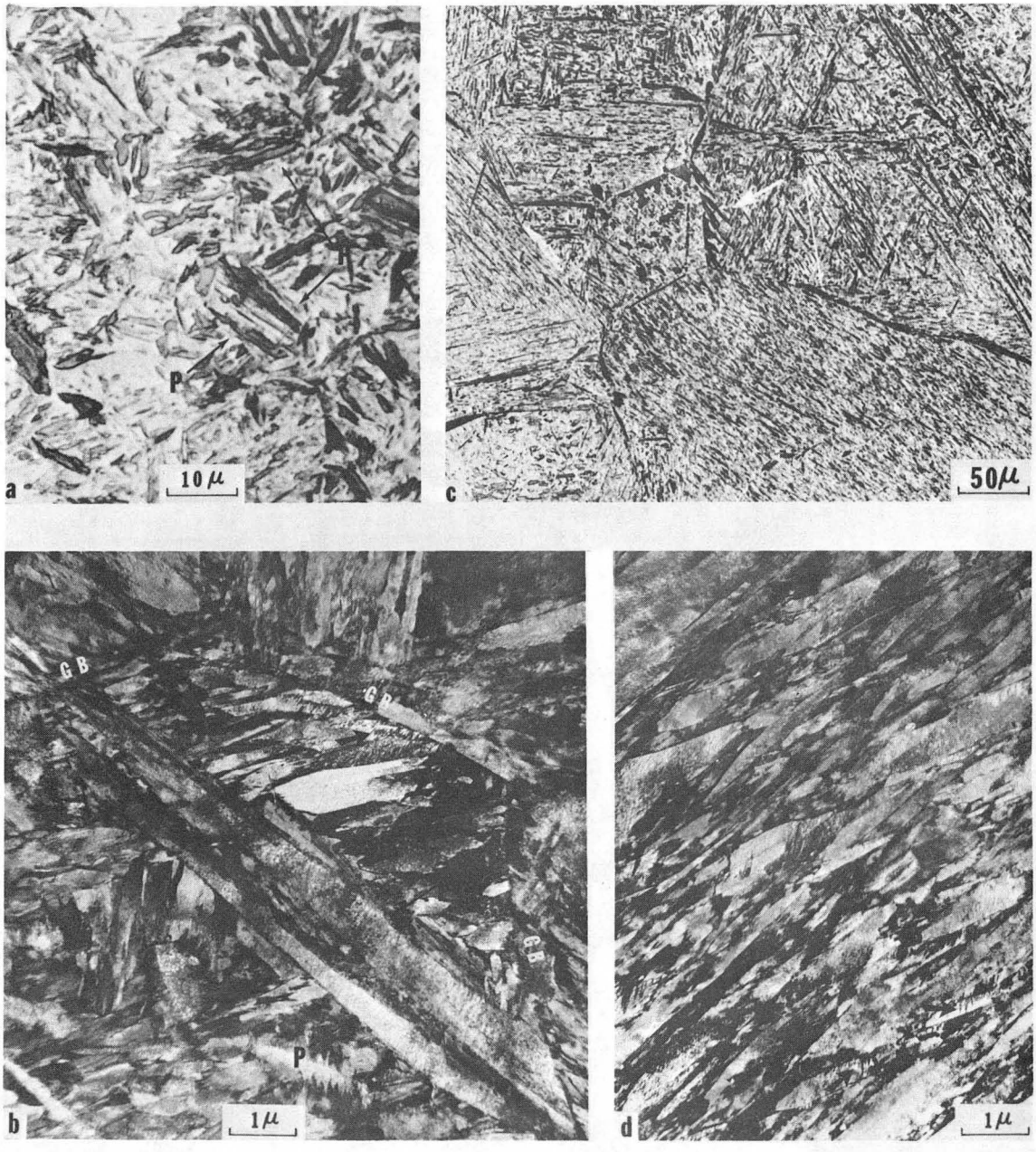

XBB 738-5014

Fig. 4

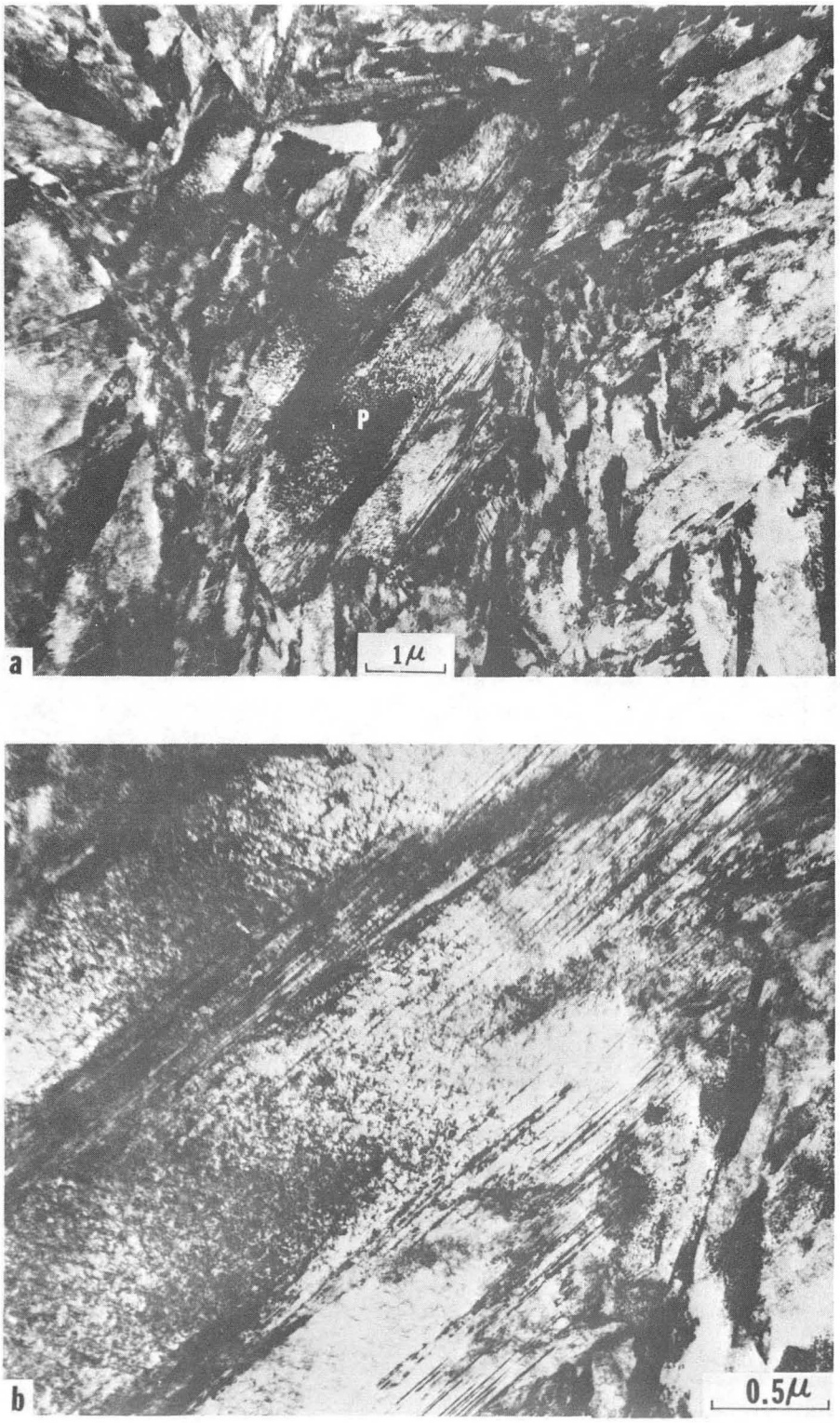

XBB 738-5018

Fig. 5

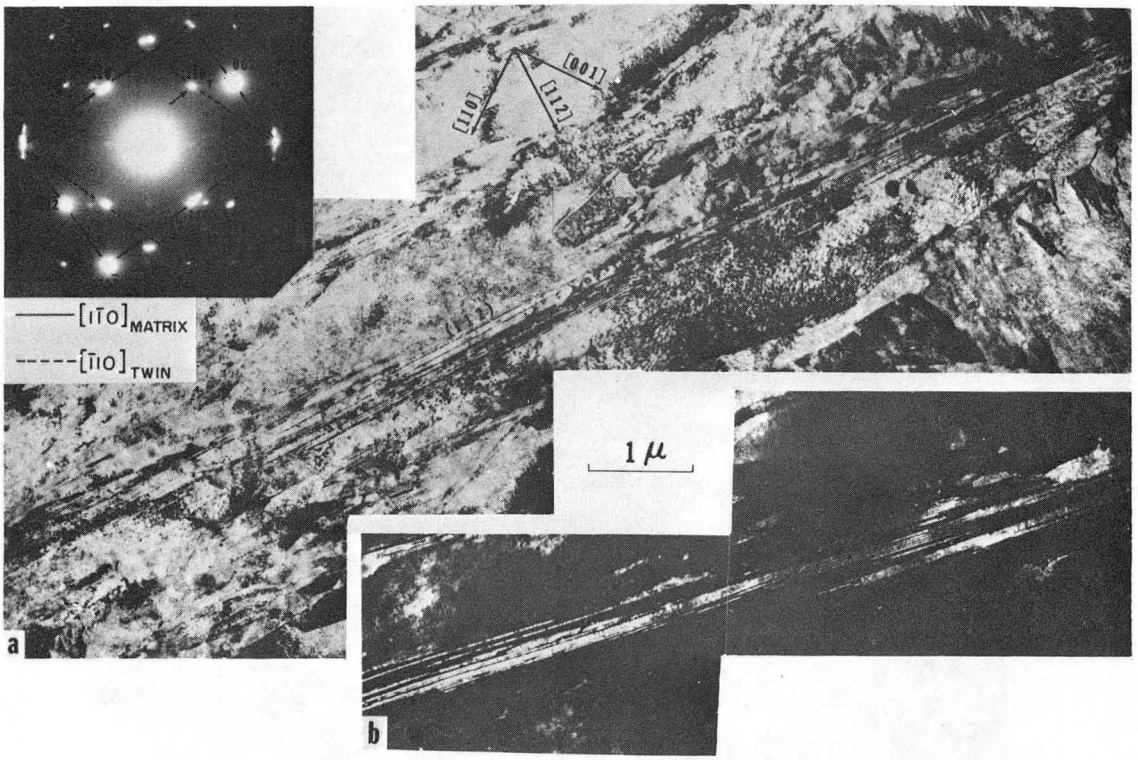

Fig. 6

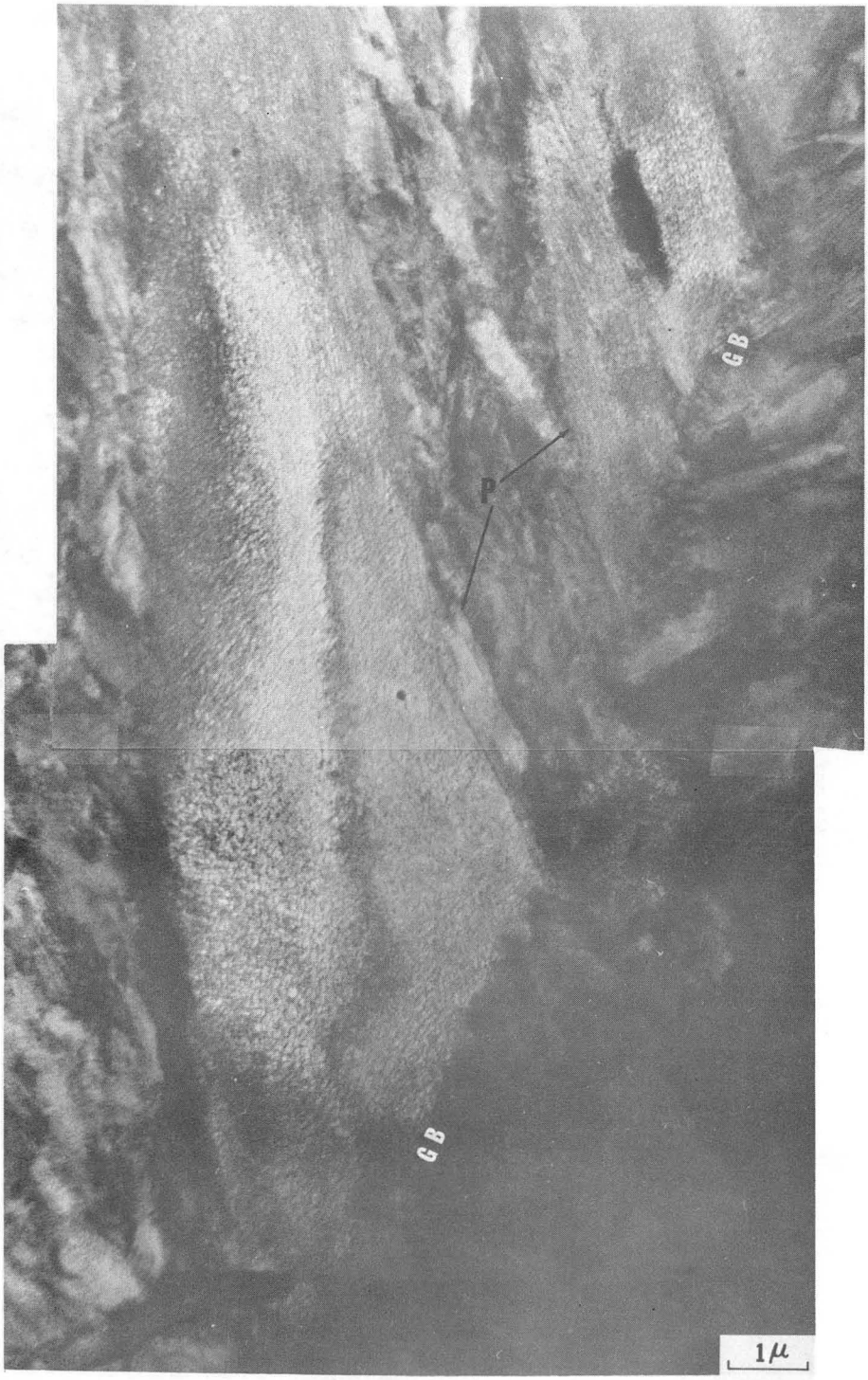

XBB 738-5028

Fig. 7

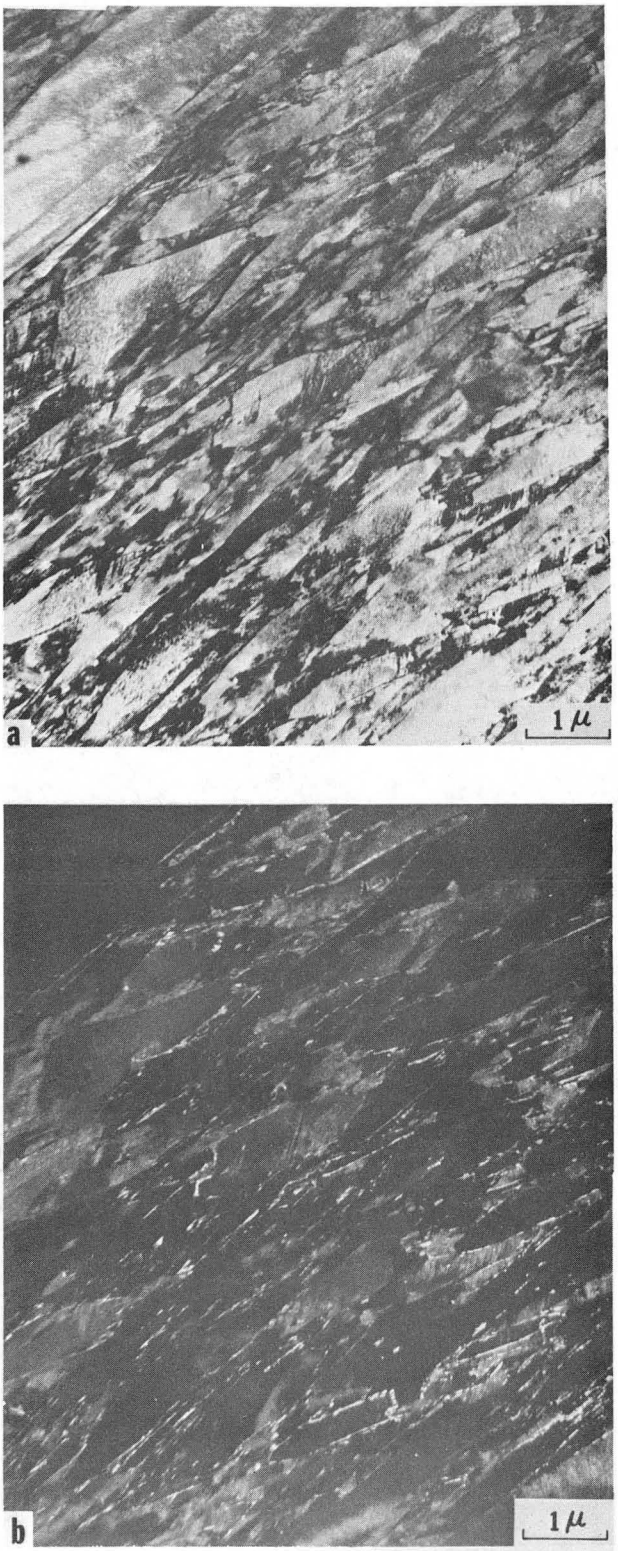

XBB 742-1250

Fig. 8

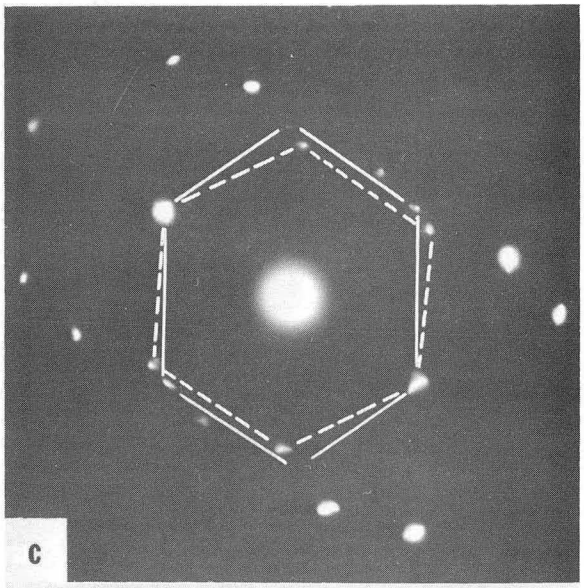
c

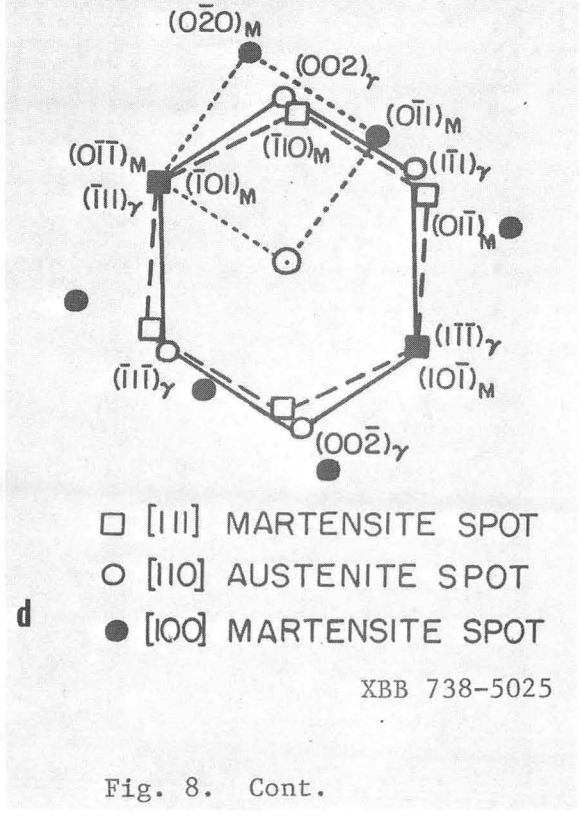
$(0\bar{2}0)_M$
$(002)_\gamma$
$(0\bar{1}1)_M$
$(\bar{1}10)_M$
$(0\bar{1}\bar{1})_M$
$(\bar{1}\bar{1}1)_\gamma$
$(\bar{1}01)_M$
$(01\bar{1})_M$
$(1\bar{1}\bar{1})_\gamma$
$(\bar{1}1\bar{1})_\gamma$
$(10\bar{1})_M$
$(00\bar{2})_\gamma$
d
□ [111] MARTENSITE SPOT
○ [110] AUSTENITE SPOT
● [100] MARTENSITE SPOT
XBB 738-5025

Fig. 8. Cont.

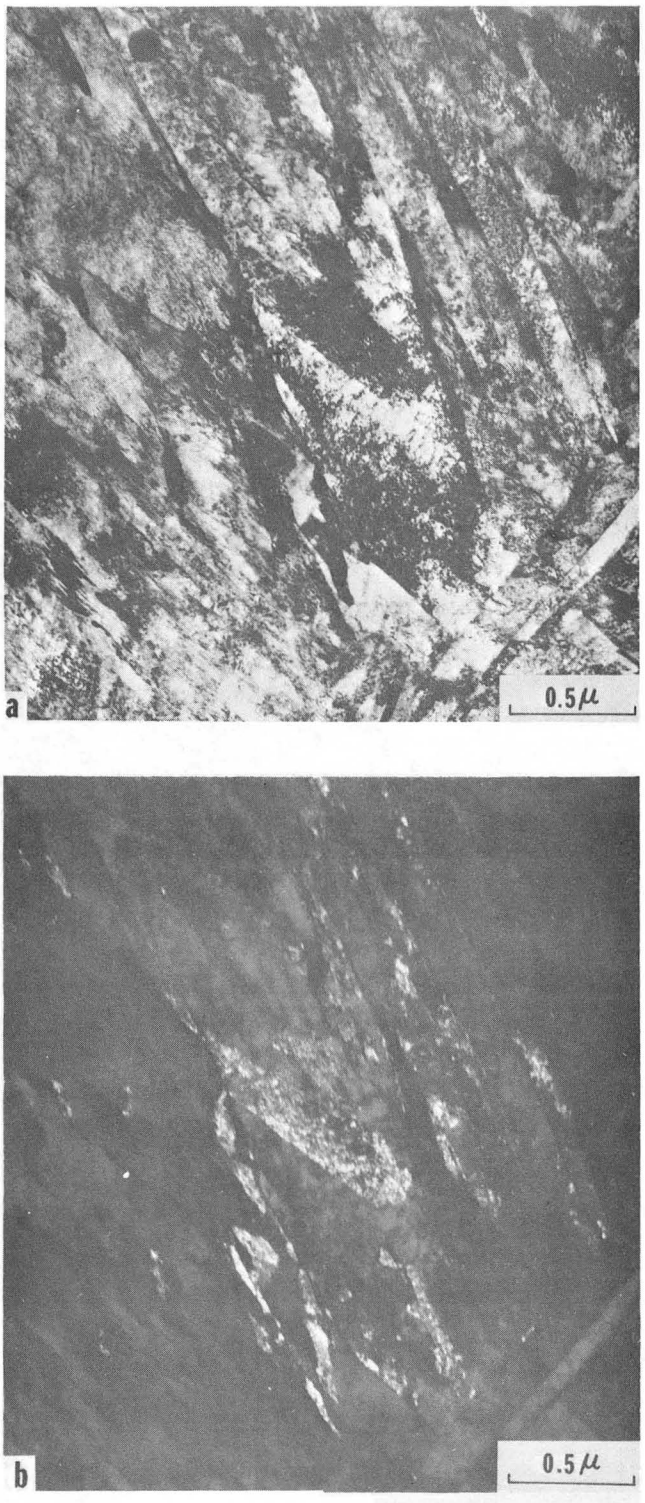

XBB 738-5021

Fig. 9

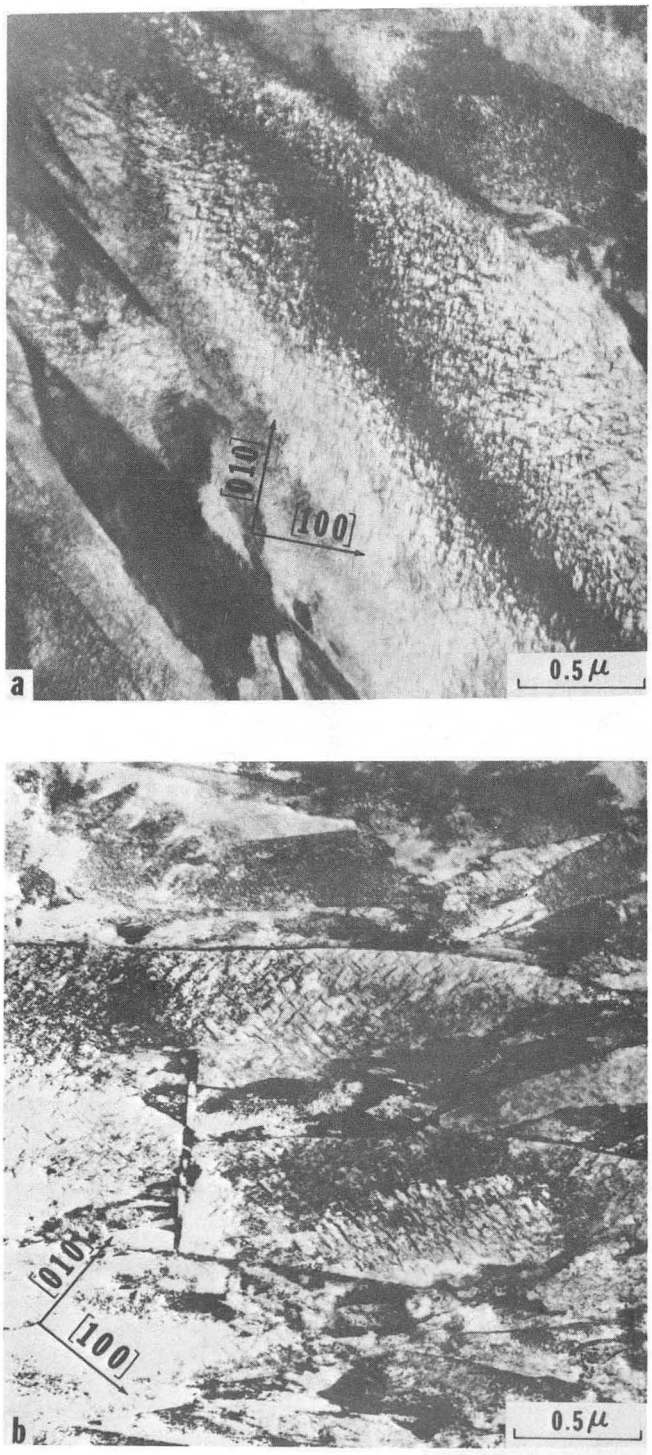

XBB 738-5022

Fig. 10

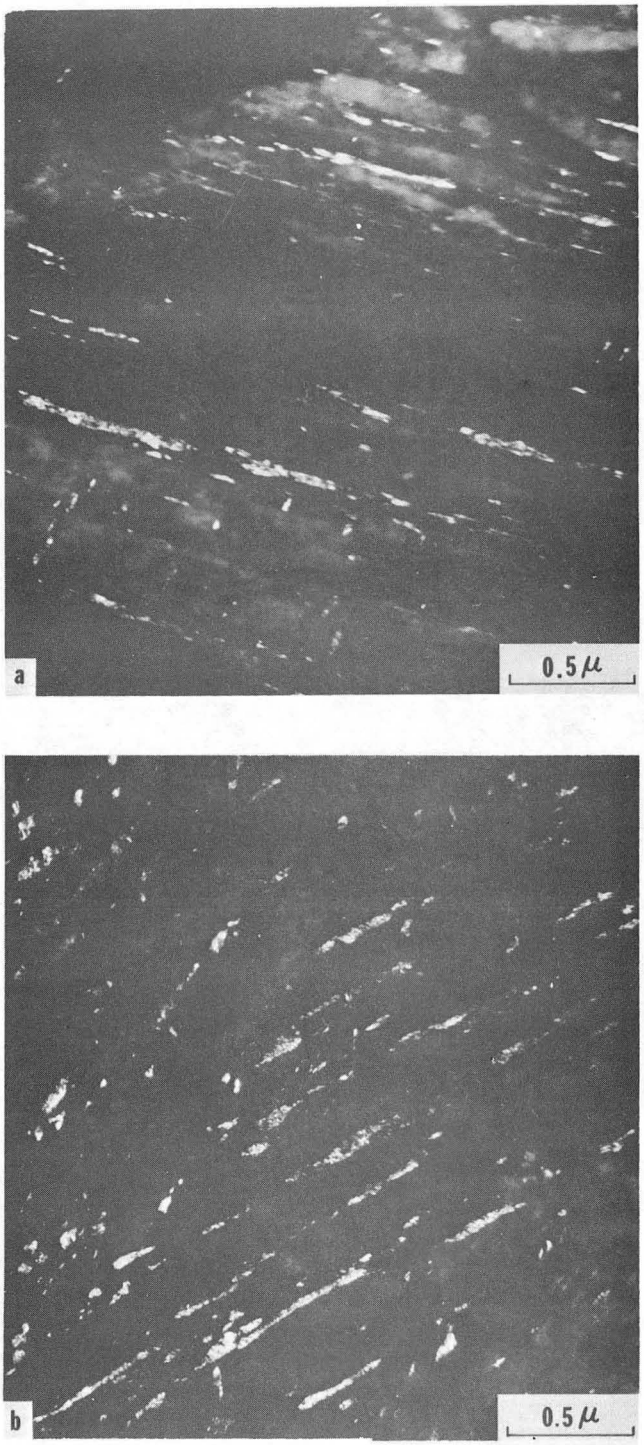

XBB 738-5023

Fig. 11

XBB 743-1694

Fig. 12

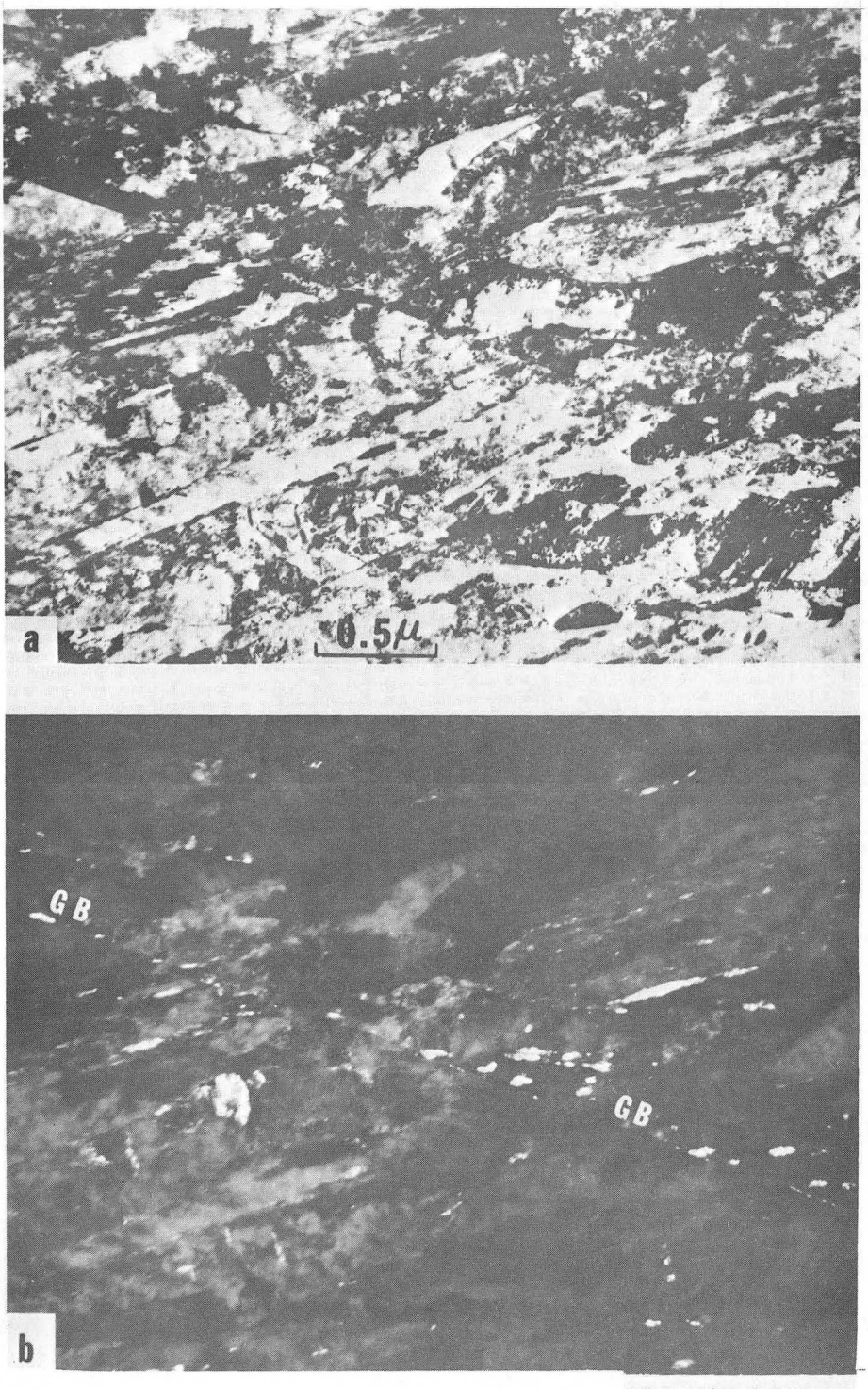

XBB 743-1695

Fig. 13

TECHNICAL INFORMATION DIVISION
LAWRENCE BERKELEY LABORATORY
UNIVERSITY OF CALIFORNIA
BERKELEY, CALIFORNIA 94720